

Multiple Linear Regression Model for Prediction of Summer Tropical Cyclone Genesis Frequency over the Western North Pacific

Ki-Seon Choi*, Yu-Mi Cha, Ki-Ho Chang, and Jong-Ho Lee

National Typhoon Center, Korea Meteorological Administration, Jeju 699-942, Korea

북서태평양 태풍발생빈도 예측을 위한 다중회귀모델 개발

최기선* · 차유미 · 장기호 · 이종호

기상청 국가태풍센터, 699-942, 제주특별자치도 서귀포시 남원읍 서성로 810번길 2

Abstract: This study has developed a multiple linear regression model (MLRM) for the seasonal prediction of the summer tropical cyclone genesis frequency (TCGF) over the western North Pacific (WNP) using the four teleconnection patterns. These patterns are representative of the Siberian high Oscillation (SHO) in the East Asian continent, the North Pacific Oscillation (NPO) in the North Pacific, Antarctic oscillation (AAO) near Australia, and the circulation in the equatorial central Pacific during the boreal spring (April-May). This statistical model is verified by analyzing the differences hindcasted for the high and low TCGF years. The high TCGF years are characterized by the following anomalous features: four anomalous teleconnection patterns such as anticyclonic circulation (positive SHO phase) in the East Asian continent, pressure pattern like north-high and south-low in the North Pacific, and cyclonic circulation (positive AAO phase) near Australia, and cyclonic circulation in the Nino3.4 region were strengthened during the period from boreal spring to boreal summer. Thus, anomalous trade winds in the tropical western Pacific (TWP) were weakened by anomalous cyclonic circulations that located in the subtropical western Pacific (SWP) in both hemispheres. Consequently, this spatial distribution of anomalous pressure pattern suppressed convection in the TWP, strengthened convection in the SWP instead.

Keywords: Multiple linear regression model, tropical cyclone genesis frequency, teleconnection pattern

요약: 이 연구는 북서태평양에서 여름철(7-9월) 동안 발생하는 태풍 빈도를 예측하기 위한 다중회귀모델을 4가지 원격 패턴을 이용하여 개발하였다. 이 패턴은 4-5월 동안 동아시아 대륙에서의 시베리아 고기압 진동, 북태평양에서의 북태평양 진동, 호주근처의 남극진동, 적도 중앙태평양에서의 대기순환으로 대표된다. 이 통계모델은 이 모델로부터 예측된 높은 태풍발생빈도의 해와 낮은 태풍발생빈도의 해 사이에 차를 분석함으로써 검증되었다. 높은 태풍발생빈도의 해에는 다음과 같은 4가지의 아노말리 특성을 나타내었다: i) 동아시아 대륙에 고기압성 순환 아노말리(양의 시베리아 고기압 진동), ii) 북태평양에 남저북고의 기압계 아노말리, iii) 호주 근처에 저기압성 순환 아노말리(양의 남극진동), iv) 봄부터 여름 동안 니노3.4 지역에 저기압성 순환 아노말리. 따라서 적도 서태평양에서 무역풍 아노말리는 양반구의 아열대 서태평양에 위치한 저기압성 순환 아노말리에 의해 약화되었다. 결국, 이러한 기압계 아노말리의 공간분포는 열대 서태평양에 대류를 억제하는 대신 아열대 서태평양에 대류를 강화시켰다.

주요어: 다중회귀모델, 태풍발생빈도, 원격패턴

*Corresponding author: choiks@kma.go.kr
Tel: +82-64-801-0230
Fax: +82-64-805-0366

This is an Open-Access article distributed under the terms of the Creative Commons Attribution Non-Commercial License (<http://creativecommons.org/licenses/by-nc/3.0>) which permits unrestricted non-commercial use, distribution, and reproduction in any medium, provided the original work is properly cited.

Introduction

Gray (1975) identified six physical parameters for TC genesis: (i) low-level relative vorticity, (ii) local or planetary vorticity (Coriolis parameter), (iii) inverse of the vertical shear of the horizontal wind between the lower and upper troposphere, (iv) ocean

thermal energy due to temperatures above 26.8°C to a depth of 60 m, (v) vertical gradient of equivalent potential temperature between the surface and 500 hPa, and (vi) middle-troposphere relative humidity. The Gray's parameters have often been used as large-scale predictors of the statistical model for seasonal prediction of the TC genesis because they were good at describing the seasonal characteristics of TC activities (DeMaria et al., 2001; Clark and Chu, 2002). When combined, in particular, it has been shown that these parameters broadly identify the geographical and seasonal distribution of tropical cyclogenesis in each of the major ocean basins. This combination of parameters is known as the *seasonal genesis parameter* (e.g., Watterson et al., 1995; Royer et al., 1998).

Poisson regression method has been an effective statistical method for the prediction of seasonal TC frequency. The advantage of the Poisson regression over linear regression is that it is more applicable for modeling the occurrence of rare, discrete events such as the TC genesis frequency (TCGF) and TC passage frequency. McDonnell and Holbrook (2004) and Chu and Zhao (2007) succeeded in predicting the TC frequency using this statistical method. These studies have also used the Gray parameters as predictors in the Poisson regression model.

As shown in the above studies, TCGF by using parameters (Gray parameters) in the TC genesis basins has been successfully predicted in many studies. However, the TC may occur through the interaction with a wide range of teleconnection patterns in the areas other than tropical region as well as by environmental factors in the tropical area (Wang and Fan, 2007; Wang et al., 2007; Choi et al., 2009; Choi and Kim, 2011a; Choi and Kim, 2011b). Therefore, it's especially important to explore the signals of the teleconnection patterns that have an impact on the TC genesis. Chan et al. (2001) used predictors of teleconnection patterns rather than the Gray's parameters. In other words, they showed that it's been successful in predicting TCGF during warm and cold events of the ENSO

in 1997 and 1998 when TCGF was abnormal using the predictors such as (i) sea surface temperature anomalies over the central and eastern Pacific, (ii) indices that represent the characteristics of the circulation over Asia and the western Pacific from April of the previous year to March of the current year, (iii) trend of the interannual variations in TC activity (climatology and persistence), and indices that represent the characteristics of the circulation in the Australian region and South Pacific. However, this study has failed to find out what impact the diverse predictors have on the TC genesis. In a statistical model, the accurate prediction of TCGF is important. However, it's more important to have complete understanding of how the predictors are related to TCGF.

The present study proposes three teleconnection patterns that have an impact on the TCGF even though they are not highly correlated with TCGF. In addition, simple mechanism on a relationship between the TCGF and the four teleconnection patterns is analyzed in this study.

Data and Method

The information about TC activity is obtained from the summer (July, August, and September) best track archives of the RSMC, Tokyo. The data sets consist of names, longitude and latitude positions, minimum surface pressures (hPa), and maximum sustained wind speeds (kt) measured every 6-hour for TCs from 1951-2009 (59 years). TCs are generally divided into four grades based on their maximum sustained wind speed (MSWS): tropical depression (TD; MSWS <34 kts), tropical storm (TS; 34 kts ≤ MSWS ≤ 47 kts), severe tropical storm (STS; 48 kts ≤ MSWS ≤ 63 kts), and typhoon (TY; MSWS ≥ 64 kts). The present study focuses not only on these four grades TCs, but also on extratropical cyclones (ECs) that transitioned from TCs. These are included because ECs inflict damage in the midlatitudes of East Asia.

The geopotential height (gpm), horizontal wind

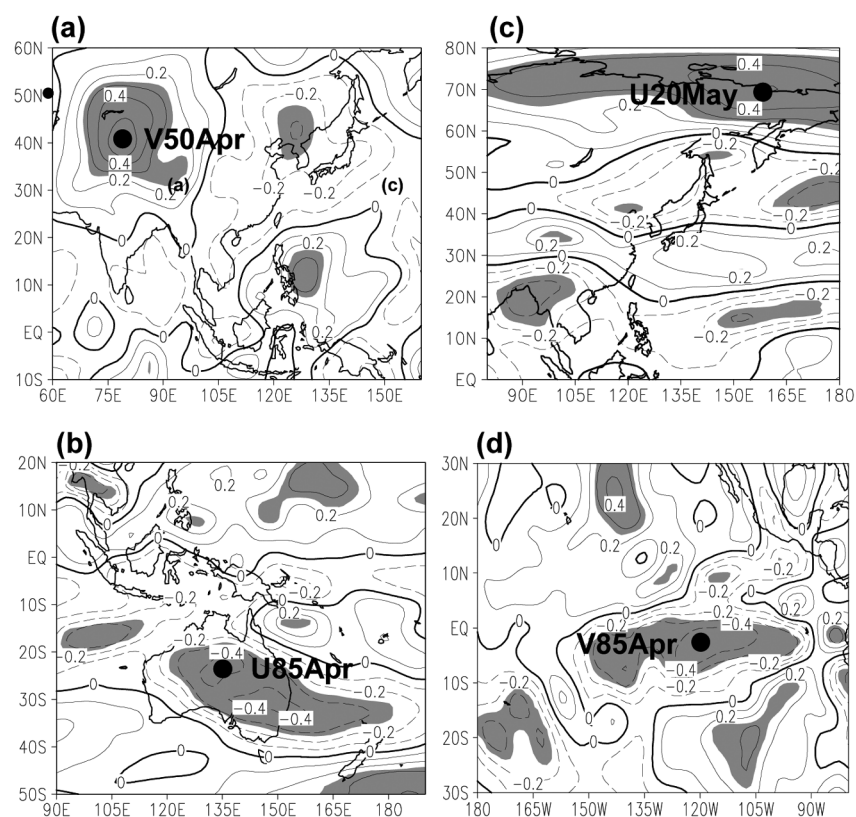


Fig. 1. Correlation coefficient map between the western North Pacific (WNP) TC genesis frequency (TCGF) during July-September (boreal summer) and (a) 500-hPa meridional wind in April, (b) 850-hPa zonal wind in April, (c) 200-hPa zonal wind in May, and (d) 850-hPa meridional wind for the period of 1951-2007. Contour interval is 0.1. Shaded area is significant at the 95% confidence level.

(ms^{-1}), and vertical velocity (hPa s^{-1}) data reanalyzed by National Centers for Environmental Prediction-National Center for Atmospheric Research (NCEP-NCAR) (Kalnay et al., 1996) were used for 59 years. These NCEP-NCAR reanalysis data have a horizontal and vertical resolutions of $2.5^\circ \times 2.5^\circ$ latitude-longitude and 17 standard pressure levels (hPa), and available for the period of 1948 to the present. Also, the monthly mean National Oceanic and Atmospheric Administration (NOAA) Extended Reconstructed SST ($^\circ\text{C}$) with $2^\circ \times 2^\circ$ grid is used.

Development of MLRM

To find the potential atmospheric circulation predictors that have an impact on TCGF during boreal summer, a correlation analysis was performed

between TCGF during boreal summer and the horizontal wind at lower (850 hPa), middle (500 hPa) and upper (200 hPa) troposphere during the preceding boreal spring (April-May) for the past 57 years. To discover the teleconnection patterns that had an impact on the TCGF in areas other than the tropical region, however, the present study has chosen the predictors based on the following procedure:

- i) Correlation coefficient of at least ± 0.45 (i.e. the points with the 99% confidence level)
- ii) To secure low correlation between predictors, the points chosen as predictors should keep certain distance between them. It is because if the independent variables that are used in the MLRM are highly correlated each other, one variable may be redundant with other variables. After all, the

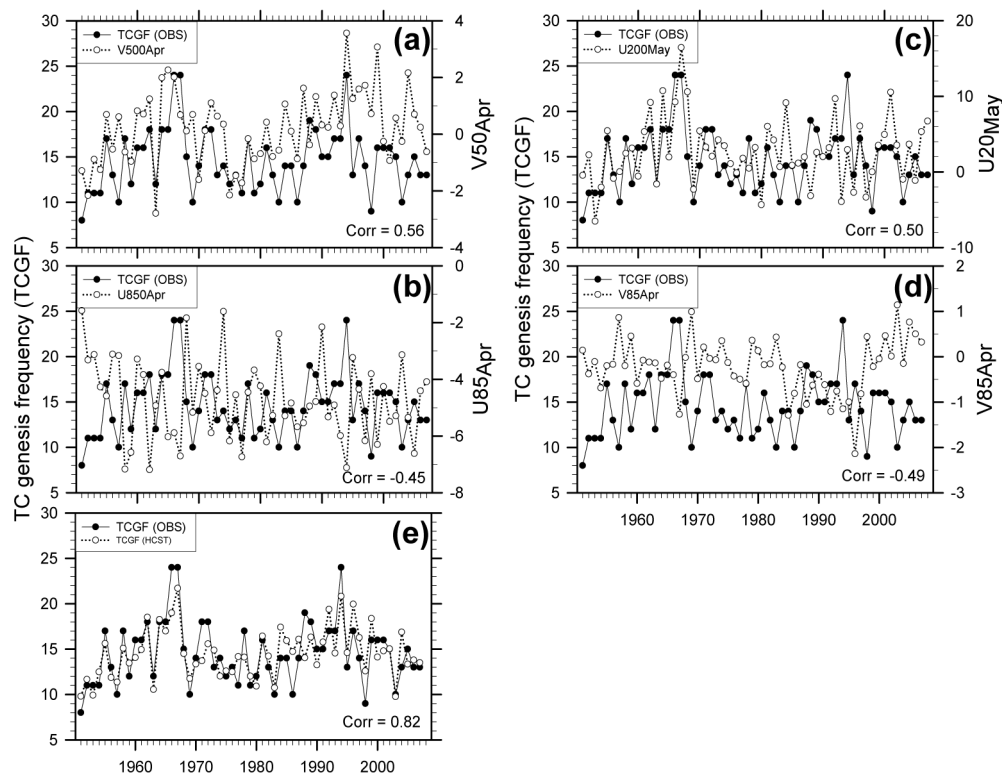


Fig. 2. Time series between the WNP TCGF during the boreal summer and values in (a) V50Apr, (b) U85Apr, (c) U20Apr, (d) V85Apr points in Fig. 1, and (e) annually observed and hindcasted TCGFs.

values predicted by the model would not be statistically significant.

Based on the aforementioned procedure, the highest correlation has been detected in three locations as shown in Fig. 1. The first predictor is meridional wind at 500-hPa level in April (Fig. 1a), which shows positive correlation near Balkhash Lake. There is a relatively low negative correlation around Korea. In other words, it can be interpreted that if anticyclone is strengthened at the middle troposphere of East Asian continent in the preceding spring, WNP TCGF would increase in summer. The second predictor is zonal wind at 850-hPa level in April (Fig. 1b), which shows high negative correlation in Australia. In the northeast of the nation, however, a positive correlation is observed. In other words, it can be interpreted that if cyclone is strengthened at the lower troposphere of Australia in the preceding spring, WNP TCGF would increase in summer. The

third predictor is zonal wind at 200-hPa level in May (Fig. 1c), which shows high positive correlation at the upper troposphere of the northeast Siberian area, and negative correlation in the south of the northeast Siberian area and then positive correlation in the farther southern part of the northeast Siberian area. In other words, it can be interpreted that if upper troposphere anticyclone and cyclone are strengthened in the North Pacific and in the south of the North Pacific respectively in the preceding spring, WNP TCGF would increase in summer. Lastly, a negative correlation to 850 hPa meridional wind in April is observed around Niño3.4 region and a positive correlation above that region (Fig. 1d). This means WNP TCGF would increase if clockwise circulation is strengthened in the Niño3.4 region.

The time series on predictors at the above three points chosen in the preceding spring and WNP

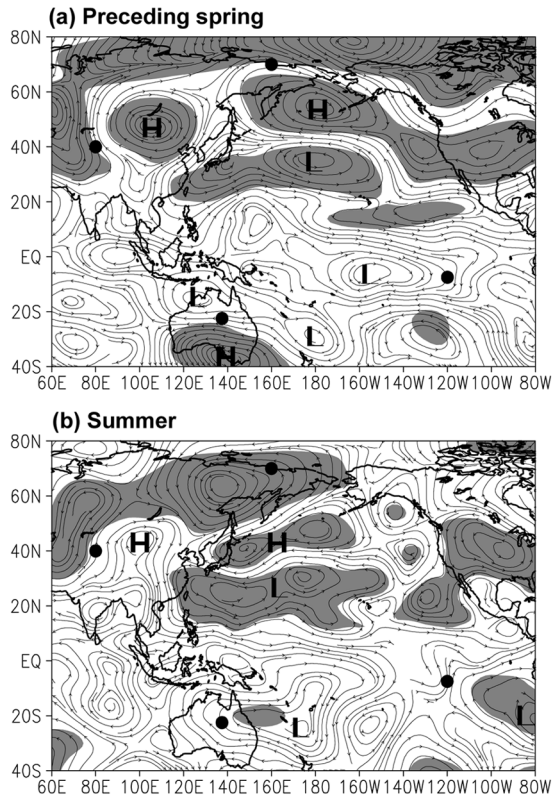


Fig. 3. Difference in tropospheric layer mean flows (TLMFs) between positive and negative years for the (a) preceding boreal spring (April-May) and (b) summer. Shade areas denote regions that is greater than the 95% level of significance.

TCGF in summer for the past 57 years are shown in Fig. 2. The time series of the four predictors relatively follow the fluctuation of TCGF. Among the four predictors, the 500-hPa meridional wind near Balkhash Lake in the preceding April shows the highest correlation (Fig. 3a). The correlation coefficients between TCGF and three predictors are significant at the 95% confidence level. The MLRM that reflects the characteristics of large-scale circulation of the above three predictors have been established as follows:

$$\begin{aligned}
 TCGF_{JA} = & 0.94 * V50_{Apr} (80.0 E, 40.0 N) \\
 & -0.59 * U85_{Apr} (137.5 E, 22.5 S) \\
 & +0.27 * U20_{May} (160.0 E, 70.0 N) \\
 & -1.79 * V85_{Apr} (120.0 W, 7.5 S) + 10.45
 \end{aligned}$$

Here, ‘ U ’ and ‘ V ’ represent zonal and meridional winds respectively while 85, 50 and 20 refer to 850, 500 and 200 hPa levels, individually. It’s already been mentioned that there should be low correlation between the predictors that compose MLRM. In the present study, no high correlation has been detected either among the three predictors (less than ± 0.2). The time series of summer TCGF which have been observed and hindcasted by MLRM are shown in Fig. 3d. The variation of hindcasted summer TCGF properly describes the fluctuation in observed summer TCGF. In addition, the values are almost same. Therefore, a high correlation is detected between the two time series at the 99% confidence level. The mean absolute error (MAE) between observed TCGF and hindcasted TCGF is 1.8. The observed and hindcasted TCGFs in 2008 and 2009 are 11 and 13.2, and 14 and 16.9, respectively.

Difference between the Hindcasted Positive and Negative TCGF Years

To synoptically examine the varification of the MLRM, as indicated in Table 1, the seventeen highest years (hereafter, positive years) and seventeen lowest years (hereafter, negative years) are selected from time series that hindcasted by the MLRM in Fig. 2e, and then the differences between the two phases are analyzed as follows. Here, the selected positive and negative years account for two thirds of the entire analysis period and have values above 0.4 and below -0.5 in the normalized time series that hindcasted by the MLRM, respectively.

Fig. 3 shows that differences in tropospheric layer mean flows (TLMFs) between positive and negative years for the preceding boreal spring (April-May) and boreal summer. In the preceding boreal spring, anomalous anticyclonic circulation is located in the East Asian continent (Fig. 3a). In this area where this anomalous circulation is, the Siberian anticyclone climatologically exists during the cold season (Jeong

Table 1. Comparison of hindcasts (HCST) and observations (OBS) for the 17 positive and negative TCGF years hindcasted by MLRM

Positive years			Negative years		
Year	OBS	HCST	Year	OBS	HCST
1962	18	18.5	1951	8	9.8
1964	18	18.3	1952	11	11.7
1965	18	17.0	1953	11	9.9
1966	24	19.0	1954	11	12.5
1967	24	21.7	1956	13	11.9
1981	16	16.4	1957	10	11.4
1984	14	17.4	1963	12	10.6
1985	14	15.9	1969	10	11.8
1987	14	16.1	1974	14	12.0
1989	18	16.3	1975	12	12.6
1991	15	15.8	1976	13	12.5
1992	17	19.4	1979	11	12.0
1994	24	20.8	1980	12	10.9
1996	17	19.9	1983	10	10.7
1997	14	16.3	1990	15	13.3
1999	16	18.4	1998	9	12.6
2004	13	16.9	2003	10	9.8
AVG	17.3	17.9	AVG	11.3	11.5
STD	3.6	1.8	STD	1.8	1.1

and Renwick, 2008). This area is similar to the zone which is applied as an index to define the variation of the Siberian anticyclone [hereinafter referred to as Siberian High Oscillation (SHO)]. Therefore, this anomalous anticyclonic circulation during the preceding spring in positive years means that the Siberian High is stronger than the mean (i.e. positive SHO phase). In the North Pacific, anomalous anticyclonic circulation is observed in high-latitudes (40° - 60° N) while anomalous cyclonic circulation is observed in mid-latitudes (20° - 40° N). In other words, north-high and south-low anomalous pressure pattern is shown, which is similar to the positive phase of the North Pacific Oscillation (NPO) (Walker and Bliss, 1932; Rogers, 1981). In particular, the anomalous cyclonic circulation which is dominant in the mid-latitudes of the North Pacific means that a WNP high (WNPH) is not developed in positive years. In the northern part of the Australia, on the other hand, anomalous low circulation is observed. This circulation ranges up to

the anomalous trough in the sea southeast of Australia. This kind of feature is similar to the negative phase of Antarctic Oscillation (AAO) (Gong and Wang, 1999). In the Niño3.4 region (0 - 20° S, 170° W- 110° W), anomalous low circulation is strengthened, which seems to be related to ENSO.

This kind of atmospheric pressure patterns which form in the preceding spring during positive and negative years are well lasted until summer. On the whole, the atmospheric pressure system is located to the south as compared the preceding spring (Fig. 3b). However, anomalous anticyclonic circulation (positive SHO phase) and north-high and south-low anomalous pressure pattern (positive NPO phase) are still observed in the northern part of China and North Pacific, respectively. Anomalous northerlies from the anomalous anticyclones in a latitude band of approximately 40° N prevail in the subtropical WNP. According to Chen et al. (1998), these anomalous flows had a positive impact on TCGF through enhancement of convection in the subtropical WNP. As to the north-high and south-low anomalous pressure pattern observed in the North Pacific, Wang et al. (2007) explored the relationship between the NPO and TCGF and then they showed that there exists a positive relationship between the two. In addition, Fan (2007) demonstrated that a condition of the sea ice that is less in the North Pacific during the preceding spring can be linked with the positive TCGF via the teleconnection pattern of the positive NPO. Meanwhile, continuous strengthening of anomalous cyclonic circulation has been observed from the north to the southeast of Australia since the preceding spring. On the other hand, anomalous cyclonic circulations around Australia are more obvious than in the preceding boreal spring. Wang and Fan (2007) also stressed that the variation of the summer WNP TCGF are negatively related to AAO via the meridional teleconnection pattern. The trough derived from anomalous cyclonic circulation over the Australian is also stretched to the Niño3.4 region.

In order to examine that circulation between the

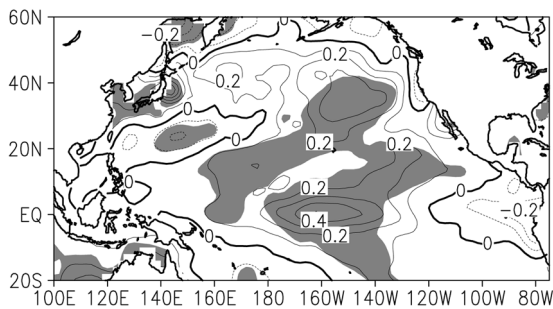


Fig. 4. Difference in sea surface temperature (SST) between positive and negative years during the boreal summer. Shade areas denote regions that is greater than the 95% the significance level. Contour interval is 0.1°C.

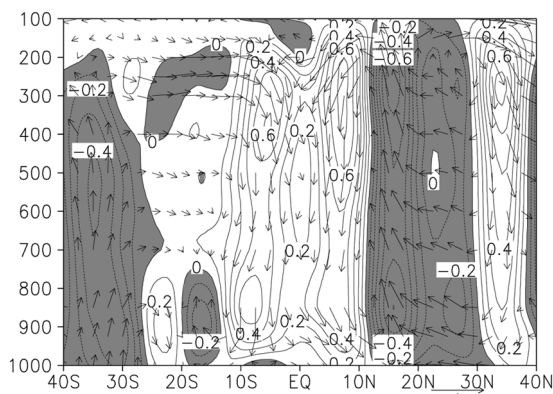


Fig. 5. Height-latitude cross section of composites of anomalies of vertical flow and vertical velocity averaged for 100-150E for a difference between the two phases during the boreal summer. Shaded areas indicate positive value for vertical velocity. Contour interval is 0.1 $\text{h} \cdot \text{Pa}^{-1}$. Vertical velocity is multiplied by 10^2 .

two phases in the Niño3.4 region is related to SST condition, the differences in SST between positive and negative years are analyzed for the boreal summer (Fig. 4). It can be confirmed that warm SST is predominant over the Niño3.4 region. This condition of SST is also observed in the preceding boreal spring (not shown). It can be related to the trade winds (westerlies) that weakened (strengthened) along equatorial region for the positive years.

Ho et al. (2005) further investigated the difference in convective activity between the two phases by analysing the characteristics of meridional vertical circulation averaged along 110°-150°E, the major TC

genesis longitude band in summer (Fig. 5). While anomalous downward flows are distinctive at 10°S-10°N in positive years, anomalous upward flows are strong at 10°-20°N in the North Hemisphere and at the north of 25°S in the South Hemisphere. In negative years, on the contrary, strong anomalous upward flows are shown at 10°S-10°N where TC genesis is hardly observed due to weak Coriolis force while anomalous downward flows are distinctive in the subtropical region of the both Hemispheres. This kind of result is equivalent to the contention of Ho et al. (2005) which insisted that the anomalous trade winds that have intensified during negative years strengthen the convection along the narrow latitude band in the western tropical Pacific only. The anomalous downward flows near the equator and anomalous upward flows at 10°-30°N that is major TC genesis latitude, are more distinctive than positive years in terms of the difference between the two phases.

Concluding Remarks

The present study has developed MLRM that predicts WNPH TCGF in summer using synoptic predictors in the preceding spring. As the synoptic predictors, wind variables with the highest correlation with summer WNP TCGF for the past 57 years have been chosen in four positions. The selected four positions are around Balkhash Lake at 500-hPa level, Australia at 850-hPa level, Northeast Siberia at 200-hPa level, and Niño3.4 region at 850-hPa during the preceding April and May.

Through differences between the 17 positive years (with the highest TCGF hindcasted by MLRM) and 17 negative years (with the lowest TCGF), the further verification of MLRM has been analyzed synoptically. As a result, the following distinctive three teleconnection patterns were observed in positive years.

- i) Anomalous anticyclonic circulation has been strengthened in East Asia (positive SHO phase).
- ii) North-high and south-low anomalous

atmospheric pressure pattern has been strengthened in the North Pacific (positive NPO phase).

iii) Anomalous cyclonic circulation has been strengthened in regions from the north Australia to the sea southeast of Australia and the Indian Ocean (negative AAO phase).

iv) Anomalous cyclonic circulation has been strengthened in Niño3.4 region (warm SST).

These kinds of teleconnection patterns on the variation of TCGF have continued from preceding spring to summer.

However, the statistical model proposed in this study still has some limitation in predicting extreme cases, in particular.

Acknowledgments

This research is supported by the project “Management of National Typhoon Center”, and “Development of technology for the short and long range typhoon forecast” in “Development and application of technology for weather forecast (NIMR-2013-B-1)” funded by Korea Meteorological Administration (KMA).

References

- Chan, J.C.L., Shi, J.E., and Liu, K.S., 2001, Improvements in the seasonal forecasting of tropical cyclone activity over the western North Pacific. *Weather and Forecasting*, 16, 491-498.
- Chen, T.C., Weng, S.P., Yamazaki, N., and Kiehne, S., 1998, Interannual variation in the tropical cyclone formation over the western North Pacific. *Monthly Weather Review*, 126, 1080-1089.
- Choi, K.S., Kang, K. R., Kim, D. W., Hwang, H. S., and Lee, S. R., 2009, A study on the characteristics of tropical cyclone passage frequency over the western North Pacific using Empirical Orthogonal Function. *Journal of Korean Earth Science Society*, 30, 721-733.(In Korea)
- Choi, K.S. and Kim, T.R., 2011a, Development of a diagnostic index on the approach of typhoon affecting Korean Peninsula. *Journal of Korean Earth Science Society*, 32, 347-359.(In Korea)
- Choi, K.S. and Kim, T.R., 2011b, Regime shift of the early 1980s in the characteristics of the tropical cyclone affecting Korea. *Journal of Korean Earth Science Society*, 32, 453-460.
- Chu, P.S. and Zhao, X., 2007, A Bayesian regression approach for predicting seasonal tropical cyclone activity over the central North Pacific. *Journal of Climate*, 20, 4002-4013.
- Chu, P.S., Zhao, X., Lee, C.T., and Lu, M. M., 2007, Climate prediction of tropical cyclone activity in the vicinity of Taiwan using the multivariate least absolute deviation regression approach. *Terrestrial Atmospheric and Oceanic Sciences*, 18, 805-825.
- Clark, J.D. and Chu, P.S., 2002, Interannual variation of tropical cyclone activity in the central North Pacific. *Journal of Meteorological Society of Japan*, 80, 403-418.
- DeMaria, M., Knaff, J.A., and Connell, B.H., 2001, A tropical cyclone genesis parameter for the tropical Atlantic. *Weather and Forecasting*, 16, 219-233.
- Fan, K., 2007, North Pacific sea ice cover, a predictor for the western North Pacific typhoon frequency? *Science China Series D: Earth Sciences*, 50, 1251-1257.
- Gong, D.Y. and Wang, S., 1999, Definition of Antarctic oscillation index. *Geophysical Research Letter*, 26, 459-462.
- Gray, W.M., 1975, Tropical cyclone genesis. Dept. of Atmospheric Science Paper 234, Colorado State University, Fort Collins, CO, 121 pp.
- Ho, C.H., Kim J.H., Kim, H.S., Sui, C.H., and Gong, D.Y., 2005, Possible influence of the Antarctic Oscillation on tropical cyclone activity in the western North Pacific. *Journal of Geophysical Research*, 110, D19104, doi:10.1029/2005JD005766.
- Jeong, Y.K. and Renwick, J.A., 2008, Locations of the Siberian high centers of action and associated propagation of wave-like Patterns in the Northern Hemisphere winter. *Asia-Pacific Journal of Atmospheric Sciences*, 44, 149-171.
- Kalnay, E., Kanamitsu, M., Kistler, R., Collins, W., Deaven, D., Gandin, L., Iredell, M., Saha, S., White, G., Woollen, J., Zhu, Y., Chelliah, M., Ebisuzaki, W., Higgins, W., Janowiak, J., Mo, K.C., Ropelewski, C., Wang, J., Leetmaa, A., Reynolds, R., Jenne, R., and Joseph, D., 1996, The NCEP/NCAR 40-Year Reanalysis Project. *Bulletin of American Meteorological Society*, 77, 437-471.
- McDonnell, K.A. and Holbrook H.J., 2004, A Poisson regression model of tropical cyclogenesis for the Australian-Southwest Pacific Ocean region. *Weather and Forecasting*, 19, 440-455.
- Rogers, J.C., 1981: The North Pacific oscillation. *International Journal of Climatology*, 1, 39-57.
- Royer, J.F., Chauvin, F., Timbal, B., Araspin, P., and Grimal, D., 1998, A GCM study of the impact of

- greenhouse gas increase on the frequency of occurrence of tropical cyclones. *Climate Change*, 38, 307-343.
- Ryan, B.F., Watterson, I.G., and Evans, J.L., 1992, Tropical cyclone frequencies inferred from Gray's yearly genesis parameter: Validation of GCM tropical climates. *Geophysical Research Letters*, 19, 1831-1834.
- Walker, G.T., and Bliss, E.W., 1932, *World Weather*. Memorial of Royal Meteorological Society, 4, 53-84.
- Wang, H.J. and Fan, K., 2007, Relationship between the Antarctic oscillation and the western North Pacific typhoon frequency. *Chinese Science Bulletin*, 52, 561-565.
- Wang, H.J., Sun, J.Q., and Fan, K., 2007, Relationships between the North Pacific Oscillation and the typhoon/hurricane frequencies. *Science in China Series D: Earth Science*, 50, 1409-1416.
- Watterson, I.G., Evans, J.L., and Ryan, B.F., 1995, Seasonal and interannual variability of tropical cyclogenesis: Diagnostics from large-scale fields. *Journal of Climate*, 8, 3052-3066.

2013년 7월 5일 접수
2013년 7월 22일 수정원고 접수
2013년 8월 14일 채택